

# Microwave Dielectric Spectrum of Vegetation—Part I: Experimental Observations

MOHAMED A. EL-RAYES AND FAWWAZ T. ULABY, FELLOW, IEEE

**Abstract**—This is the first paper in a two-part sequence that evaluates the microwave dielectric behavior of vegetation material as a function of water content, microwave frequency, and temperature. Part I presents experimental measurements of the dielectric spectrum from 0.2 to 20 GHz for various types of vegetation material including leaves, stalks, and trunks at various moisture conditions. The measurements were acquired using a coaxial probe technique suitable for measuring the dielectric constant of both thick materials, such as tree trunks, and thin materials, such as leaves.

In Part II, the experimental data are used to guide the development of a dual-dispersion dielectric model that incorporates the dielectric properties of water in both “free” and “bound” forms.

## I. INTRODUCTION

THE DIELECTRIC properties of vegetation material play a central role in the coupling between the electromagnetic properties of a vegetation canopy and its physical properties. The dielectric constant of a leaf, for example, is governed by its water content and salinity. In turn, the dielectric constants, shapes, and orientations of the vegetation elements together control the scattering and emission by the canopy. Despite its fundamental importance, however, the dielectric behavior of vegetation is not well understood, particularly in the microwave region. This is attributed to two factors: 1) very few microwave measurements of the dielectric constant  $\epsilon$  of vegetation have been reported to date, as reviewed in [1], and 2) the dielectric mixture models currently in use [2] to relate the dielectric constant of vegetation to the dielectrics of its constituents—the bulk vegetation material and liquid water—are quite simplistic in form and capable of providing approximate estimates at best.

The purpose of the present study is to: 1) use a broadband measurement technique to document the dielectric behavior of vegetation material over a wide frequency range, 2) examine the temperature dependence of  $\epsilon$ , and 3) develop a dielectric dispersion model based on the physical properties of the vegetation constituents. To this end, coaxial probes were developed and used in conjunction with a reflectometer system to measure the dielectric constant of both thin (such as leaves) and thick (such as

trunks) vegetation samples over the range 0.2–20 GHz. The results are presented in a two-part series: Part I, this paper, describes the measurement system, proposes a technique for measuring the dielectric constant of thin slabs, and presents dielectric spectra for several vegetation types and plant parts under a variety of moisture and temperature conditions. In Part II, which follows, a new double-dispersion mixture model is proposed and its performance is evaluated in terms of some of the data presented in this paper.

## II. MEASUREMENT SYSTEM

The dielectric data reported in this study are based on measurements of the amplitude and phase of the reflection coefficient of a coaxial probe terminated in the material under test. The system (Fig. 1) consists of a swept RF source, a network analyzer (HP 8410C), and associated couplers and data processing instrumentation. Fig. 2(a) shows a cross section of the probe tip and the dimensions of two of the probes used in this study. The operation of open-ended coaxial lines to measure the dielectric constant of unknown materials is well-documented in the literature [3]–[5]. The input reflection coefficient at the probe tip  $\rho$  is given by

$$\rho = \frac{Z_L - Z_0}{Z_L + Z_0} = \frac{Y_0 - Y_L}{Y_0 + Y_L} \quad (1)$$

where  $Y = 1/Z$ ,  $Z_0$  is the line impedance, and  $Z_L$  is the load impedance, which is governed by the geometry of the probe tip and the dielectric constant of the material it is in contact with or immersed in (for liquid materials). In general, an open-ended coaxial line may be described by an equivalent circuit of the form shown in Fig. 2(b). When placed in contact with a homogeneous material whose thickness is sufficient to simulate a slab of infinite electrical thickness, an open coaxial line has an admittance  $Y_L(\omega, \epsilon)$  given by

$$Y_L(\omega, \epsilon) = Y_i(\omega) + Y_e(\omega, \epsilon) \quad (2)$$

where  $Y_i(\omega) = j\omega C_i$  is the “internal” admittance corresponding to the fringing capacitance  $C_i$  that accounts for the fringing field in the Teflon region between the inner and outer conductors of the line. The “external” admittance  $Y_e$ , which is a function of both  $\omega$  and the complex dielectric constant  $\epsilon$  of the material under test, consists of a frequency-dependent capacitor  $C(\omega, \epsilon)$  in parallel with

Manuscript received February 24, 1987; revised June 2, 1987. This work was supported by the NASA Goddard Space Flight Center under Contract NAG 5-480.

The authors are with the Radiation Laboratory, Department of Electrical Engineering and Computer Science, The University of Michigan, Ann Arbor, MI 48109-2122.

IEEE Log Number 8716095.

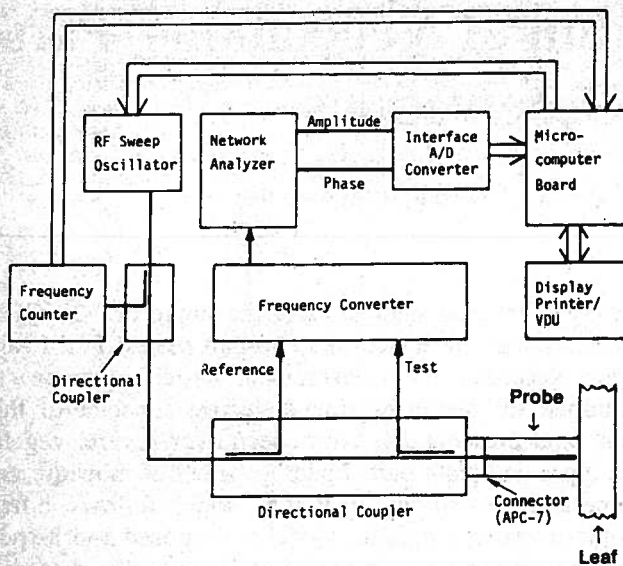


Fig. 1. Block diagram of probe dielectric system. Frequency coverage is 0.1–20 GHz.

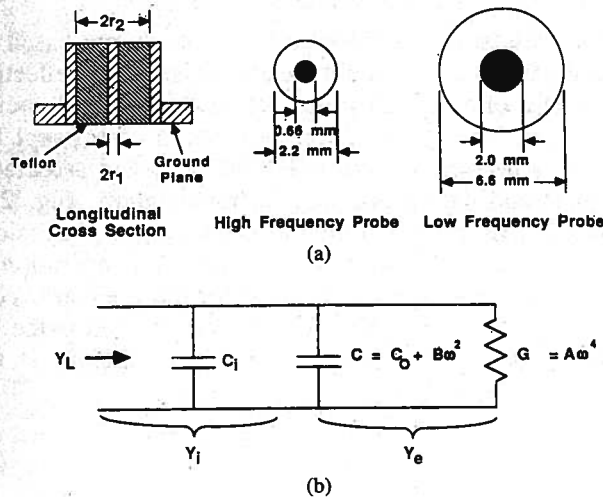


Fig. 2. (a) Coaxial probe, and (b) its equivalent circuit.

a radiation conductance  $G(\omega, \epsilon)$

$$Y_e(\omega, \epsilon) = j\omega C(\omega, \epsilon) + G(\omega, \epsilon). \quad (3)$$

The capacitor  $C(\omega, \epsilon)$  represents the fringing field concentration in the dielectric medium ( $\epsilon$ ) surrounding the probe tip, and the conductance  $G(\omega, \epsilon)$  represents the radiation into the dielectric medium.

When the medium surrounding the probe tip is free space (i.e., an open-ended line), these two equivalent-circuit elements vary according to [3], [6, p. 213]

$$C(\omega, \epsilon_0) = C_0 + B\omega^2 \quad (4)$$

$$G(\omega, \epsilon_0) = A\omega^4 \quad (5)$$

where  $C_0$ ,  $B$ , and  $A$  are constants for a given probe-tip geometry. If the radial dimensions of the coaxial line (namely,  $r_1$  and  $r_2$ ) are small compared to the wavelength  $\lambda$ , computations using the expressions given in Marcuvitz [6] yield values for  $A$  and  $B$  that are sufficiently small that the external admittance may be approximated as  $Y_e(\omega, \epsilon_0)$

$\cong j\omega C_0$ . If the dielectric constant of the medium surrounding the probe tip is not the free space value  $\epsilon_0$ , however, the above simplification may lead to unacceptably large errors. Hence, in the general case we have

$$Y_e(\omega, \epsilon_0) = j\omega(C_0 + B\omega^2) + A\omega^4. \quad (6)$$

According to the theorem developed by Deschamps [7], the input admittance of an antenna immersed in a medium of complex dielectric constant  $\epsilon$  is related to the input admittance in free space through

$$Y_e(\omega, \epsilon) = \sqrt{\frac{\epsilon}{\epsilon_0}} Y_e\left(\omega \sqrt{\frac{\epsilon}{\epsilon_0}}, \epsilon_0\right). \quad (7)$$

The above expression is for materials characterized by  $\mu = \mu_0$ . If we regard the open-ended coaxial line as an antenna and henceforth abbreviate the relative dielectric constant ratio  $\epsilon/\epsilon_0$  as simply  $\epsilon$ , we can write the following expression for the total input admittance of the probe when placed in contact with a material of relative dielectric constant  $\epsilon$ :

$$Y_L(\omega, \epsilon) = j\omega C_i + j\omega C_0\epsilon + jB\omega^3\epsilon^2 + A\omega^4\epsilon^{2.5}. \quad (8)$$

With the line admittance  $Y_0$  known, measurements of the amplitude and phase of  $\rho$  by the network analyzer system (Fig. 1) lead to a measurement of  $Y_L$ . The next step is to determine  $\epsilon$  from  $Y_L$ . This is accomplished by 1) calibrating the measurement probe in order to establish the values of the constants  $C_i$ ,  $C_0$ ,  $B$ , and  $A$ , and 2) developing an iterative program for finding a value for  $\epsilon$  that minimizes the error between the measured value of  $Y_L$  and the value calculated from the expression on the right-hand side of (8).

#### A. Usable Frequency Range

The radii  $r_1$  and  $r_2$  of the coaxial line govern three important characteristics of the dielectric measurement system:

1) The ratio  $r_1/r_2$  determines the characteristic impedance  $Z_0$  of the line. For 50- $\Omega$  Teflon-filled lines, this ratio is approximately 0.3.

2) The difference  $(r_2 - r_1)$  determines the cutoff wavelength of the TM modes [6, p. 74]; the cutoff wavelength of the  $TM_{01}$  modes is  $\lambda_c \cong 2(r_2 - r_1)$ . Table I provides a list of the dimensions and cutoff wavelengths of four standard coaxial lines used in this study. For a medium with a complex dielectric constant  $\epsilon = \epsilon' - j\epsilon''$ , the wavelength in the medium  $\lambda_\epsilon$  is related to the wavelength in free space  $\lambda_0$  by

$$\lambda_\epsilon = \lambda_0 \left[ \frac{\epsilon'}{2} (1 + \sec \delta) \right]^{-1/2} \quad (9)$$

where  $\delta = \tan^{-1}(\epsilon''/\epsilon')$ . To avoid the propagation of TM modes, the condition  $\lambda_\epsilon < \lambda_c$  should be satisfied. Table II provides values of  $\lambda_\epsilon$  for distilled water at a selected set of frequencies. If we regard distilled water as a material whose dielectric properties represent the upper end of the range of dielectric values of materials to be

TABLE I  
DIMENSIONS AND CUTOFF WAVELENGTH  $\lambda_c$  FOR THE TM<sub>01</sub> MODE FOR FOUR  
STANDARD-SIZE COAXIAL CABLES

Cable	Type	$r_2$ (mm)	$r_1$ (mm)	$r_2/r_1$	$\lambda_c$ (mm)
0.09"	Teflon	0.84	0.26	3.28	1.18
0.14"	Teflon	1.50	0.46	3.30	2.13
0.25"	Teflon	2.66	0.82	3.22	3.76
0.35"	Teflon	3.62	1.12	3.22	5.07

TABLE II  
WAVELENGTH IN DISTILLED WATER AT 22°C

f(GHz)	1.0	2.0	4.0	6.0	9.0	10.0	20.0	30.0	40.0
$(\lambda_c)_c$ (mm)	33.7	16.9	11.7	5.825	4.05	3.70	2.21	1.75	1.49

tested, then both the 0.14-in probe and the 0.085-in probe are appropriate for measuring the dielectric properties of vegetation materials at frequencies below 20 GHz.

3) The probe translates variations in the dielectric constant of the test material into variations in the measured amplitude  $\rho_0$  and phase  $\phi$  of the reflection coefficient (i.e.,  $\rho = \rho_0 e^{j\phi}$ ). The variation in the measured phase depends on  $\epsilon''$  as well as  $\epsilon'$ . However, the effects of  $\epsilon''$  on  $\Delta\phi$  are of less importance compared to the effects of  $\epsilon'$  [5]. The phase sensitivity to  $\epsilon'$  may be defined as

$$S_{\epsilon'}^{\phi} = \frac{\epsilon'}{\phi} \frac{\partial \phi}{\partial \epsilon'} \quad (10)$$

and similar definitions may be given for the phase sensitivity to  $\epsilon''$  and the amplitude sensitivities to  $\epsilon'$  and  $\epsilon''$ . For a material with known  $\epsilon'$  and  $\epsilon''$ , it is possible to choose the probe size to optimize the measurement sensitivities, and hence the measurement accuracy [5]. In general, however, if the probe is to be used to measure  $\epsilon$  for a variety of different materials, it is advantageous to use the largest possible probe because the phase and amplitude sensitivities generally increase with increasing probe dimensions.

As a compromise between the need to operate over a wide frequency range extending up to 20 GHz—which requires the use of probes with small radii—and the need to have strong sensitivities to variations in  $\epsilon'$  and  $\epsilon''$ , which requires the use of probes with large radii, we used the 0.141-in probe for making measurements from 0.7 to 20 GHz and the 0.25-in probe for measurements from 0.1 to 2 GHz.

### B. Calibration

Calibration entails finding the values of the constants  $C_i$ ,  $C_0$ ,  $B$ , and  $A$  of (8) for each probe used in this study. Under ideal circumstances, one needs to determine these constants only once and at only one frequency. The equivalent-circuit model, however, is only approximate; hence, it is necessary to determine these constants at each frequency that the probe is intended to be used. For example, it was found that the constant  $A$  varies approximately at  $1/\omega$ , which means that the conductance term  $G(\omega)$  varies as  $\omega^3$ , not  $\omega^4$ .

Each dielectric probe was calibrated by measuring the complex reflection coefficient under four termination conditions: 1) short circuit, 2) open circuit, 3) probe immersed in distilled water, and 4) probe immersed in methanol. Distilled water and methanol were used because their dispersion spectra are well known [8], [9].

Numerous tests were conducted to evaluate the measurement accuracy and precision of the dielectric system. An example is shown in Fig. 3 that compares the measured dielectric spectrum of butanol to its theoretical relaxation spectrum as reported in the literature [10]. The measured values of  $\epsilon$  are in good agreement with the calculated spectrum. Based on this and other tests for both liquid and solid samples, the coaxial probes were found to have a relative accuracy of 5 percent for  $\epsilon'$  and 10 percent for  $\epsilon''$ .

### C. Thin-Sample Measurements

In the preceding discussion, the sample under test was assumed to be electrically infinite in depth. To evaluate the effective penetration depth of the probe, experiments were conducted for slabs of various thicknesses. Fig. 4 is an illustrative example of the results obtained using the 0.141-in probe; three curves are shown, one depicting the permittivity of paper when measured against a metal background (but calculated as if the paper layer were infinitely thick), another measured and calculated in a similar fashion but with Plexiglas as the background, and a third (dashed curve) measured for a very thick stack of papers (representing the true value of  $\epsilon'$ ). We observe that the curves corresponding to the measurements for paper-over-metal and paper-over-Plexiglas approach the third curve to within  $\Delta\epsilon' = 0.1$  when the thickness exceeds 3 mm. These results are based on measurements made for a low-loss material (paper) at 1 GHz. At higher frequencies and/or for lossier materials, the effective penetration depth was found to be significantly less than 3 mm. Additionally, the probe size also is a factor; as a rule of thumb, it was found that the sample thickness should be at least equal to, and preferably larger than, the radius of the probe's outer conductor.

The 3-mm thickness requirement is easy to satisfy for many materials but not for naturally thin materials such as a single leaf of vegetation. Typical leaf thickness is about 0.1 mm, thereby necessitating that a stack of 30 closely packed leaves be formed for making the dielectric measurements. It is important that the stack be under sufficient pressure to ensure that no air gaps are present between adjacent leaves.

An alternative technique was developed that allows direct measurements of thin materials. Suppose the probe is used to make a measurement of the input admittance when it is terminated with a thin dielectric slab of thickness  $d$  placed against a background consisting of an electrically thick material with dielectric constant  $\epsilon_1$ . Suppose that a second measurement is made using the same thin dielectric slab, but this time placed against a different background of dielectric constant  $\epsilon_2$ . Let us denote these mea-



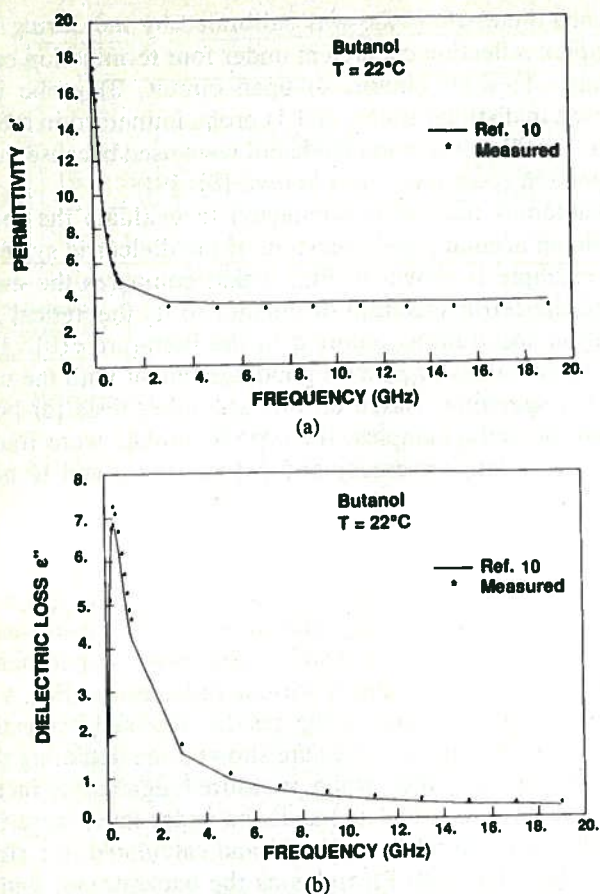


Fig. 3. Comparison of measured dielectric spectrum of Butanol to that calculated according to the dispersion equation given by Bottreau *et al.* [10]. (a)  $\epsilon'$ . (b)  $\epsilon''$ .

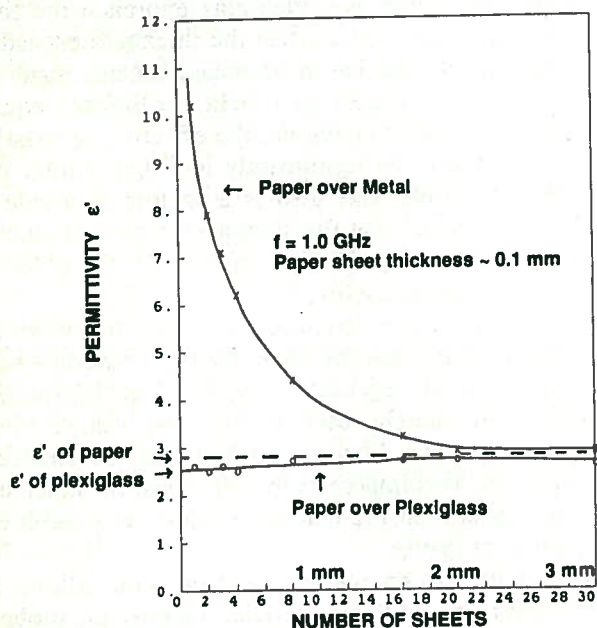


Fig. 4. Measured permittivity of paper as a function of thickness.

measurements  $Y_{L1}$  and  $Y_{L2}$ , respectively. Fig. 5 shows the prescribed arrangement with the first background material chosen to be a metal block. If the arrangement is treated as a transmission line problem, it is easy to express  $Y_{L1}$  in

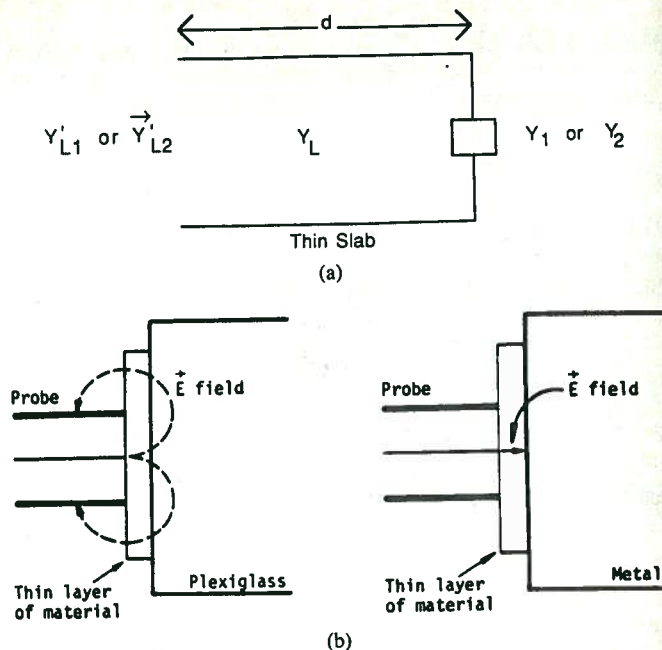


Fig. 5. Probe technique for measuring the dielectric of thin slabs; (a) transmission-line equivalent circuit of the configurations shown in (b).

terms of the unknown admittance of the thin slab  $Y_L$ , the terminating admittance  $Y_1$  of the material with dielectric  $\epsilon_1$ , and the propagation function  $\gamma d$  of the thin slab (where  $\gamma$  is the propagation constant of the slab material and  $d$  is its thickness). Similarly,  $Y_{L2}$  can be expressed in terms of  $Y_L$ ,  $Y_2$ , and  $\gamma d$ . If we eliminate  $\gamma d$  from the two expressions and choose  $Y_2 = \infty$  (metal background), we obtain the simple expression

$$Y_L = [Y_{L1} Y_{L2} + Y_1 (Y_{L1} - Y_{L2})]^{1/2}. \quad (11)$$

In the above expression  $Y_L$  represents the characteristic admittance of the thin slab, which is the load admittance that the probe would measure had the slab been infinitely thick.

The validity of this semi-empirical approach was evaluated over a wide range of frequencies for a wide range of dielectric values. In all cases the two materials used for background were metal and Plexiglas. The evaluation consisted of comparing  $\epsilon_{\text{thick}}$  as measured directly for a very thick slab with  $\epsilon_{\text{thin}}$  as measured for a very thin slab of the same material following the approach described above. The technique was found to yield satisfactory results as demonstrated by the comparison shown in Fig. 6 for 8 GHz. Similar results were obtained at other frequencies.

#### D. Sample Preparation and Handling

Solid samples are difficult to measure with the open coax method because the apparent reflection often depends on the quality of contact between the probe and the sample. Surface preparation of solid samples must be done very carefully to insure that no air gaps remain where the probe is applied. With rocks, the surface should be polished smooth prior to measurement. With semi-solid bo-

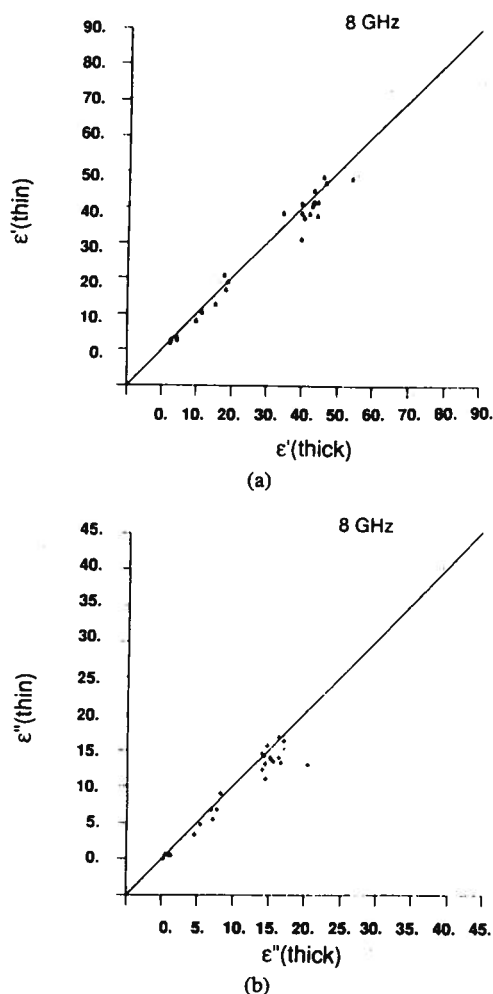


Fig. 6. Comparison of dielectric measurements made for a thick stack of corn leaves ( $\epsilon'$  thick,  $\epsilon''$  thick) with measurements made for individual leaves ( $\epsilon'$  thin,  $\epsilon''$  thin) using the technique described in the text. (a) Equivalent circuit. (b) Probe against thin layer with two different back-grounds.

tanical samples, excess pressure from the probe can crush the cellular structure beneath the probe, thereby changing the dielectric properties of the material being measured. In the present investigation, a pressure gauge was used to insure that the pressure was sufficient to result in good contact between the probe and the botanical sample but not too strong to crush the sample.

### III. EXAMPLES OF DIELECTRIC MEASUREMENTS

Over the past two years, the dielectric probe has been used to measure the dielectric spectra of many types of vegetation material under a variety of conditions. A few illustrative examples are presented in this section.

#### A. Balsam Fir Tree Trunk

The dielectric spectrum shown in Fig. 7(a) was measured by placing the dielectric probe against a flat cross section of a trunk section of a balsam fir tree. The volumetric moisture  $M_v$  of the wood was calculated from weight measurements (prior to and after oven drying) and density determination to be 0.17. Measurements made for

other trunk samples have ranged from around 0.1 for naturally dried wood to about 0.6 for freshly cut trunks. Correspondingly, the dielectric spectra vary over a wide range of values; at 5 GHz, for example,  $\epsilon'$  varies from a low value of 3.5 to a high value of 20.

#### B. Poplar Tree Trunk

An experiment was conducted to evaluate the radial variation of the dielectric constant of freshly cut tree trunks. An example of the results is sketched in Fig. 7(b) in the form of five concentric rings. Each ring contains the average dielectric constant (of 16 sample measurements made at different locations within that ring) and its average gravimetric moisture content. We observe that  $\epsilon$  decreases from 32-j8 at the center to 8-j1 at the outermost ring; actually, the measurements for this outermost ring, which consisted of the tree bark, were made from the side rather than from the top. The gravimetric moisture constant, on the other hand, is essentially the same for all rings. The radial variation of  $\epsilon$  is attributed to variation in volumetric moisture content  $M_v$ , which is related to the gravimetric moisture constant  $Mg$  through

$$M_v = \frac{Mg\rho}{1 - Mg(1 - \rho)} \quad (12)$$

where  $\rho$  is the dry density of the soil material. For a fixed value of  $Mg$ ,  $M_v$  increases with increasing  $\rho$ . For many types of trees, including the poplar variety, the density of the trunk material is highest at the center and decreases radially outward. In all physically based dielectric mixture models [8], the concentration parameters driving the model usually are the volume fractions of the constituents, not their weights.

#### C. Aspen-Leaves

Three sets of spectra are presented in Fig. 8, corresponding to leaves of aspen measured at three gravimetric moisture conditions ranging from 0.20 to 0.86 by wet weight. The spectra cover only the 1–8.5 GHz range because they were made before the system's frequency range was expanded to 20 GHz.

#### D. Corn Leaves and Stalks

Fig. 9 presents a family of dielectric spectra for corn leaves, measured at several gravimetric moisture conditions extending from 0.83 (freshly cut) down to 0.08. The data were used in the development of the models discussed in Part II. Similar dielectric data were measured for corn stalks and found to exhibit a moisture dependence very similar to that exhibited by the dielectric constant of leaves.

#### E. Corn Stalk Fluid

Pressure techniques were used to extract samples of the fluids contained in some of the vegetation materials examined in this study. Fig. 10 shows the spectrum measured by the dielectric probe for a fluid sample extracted

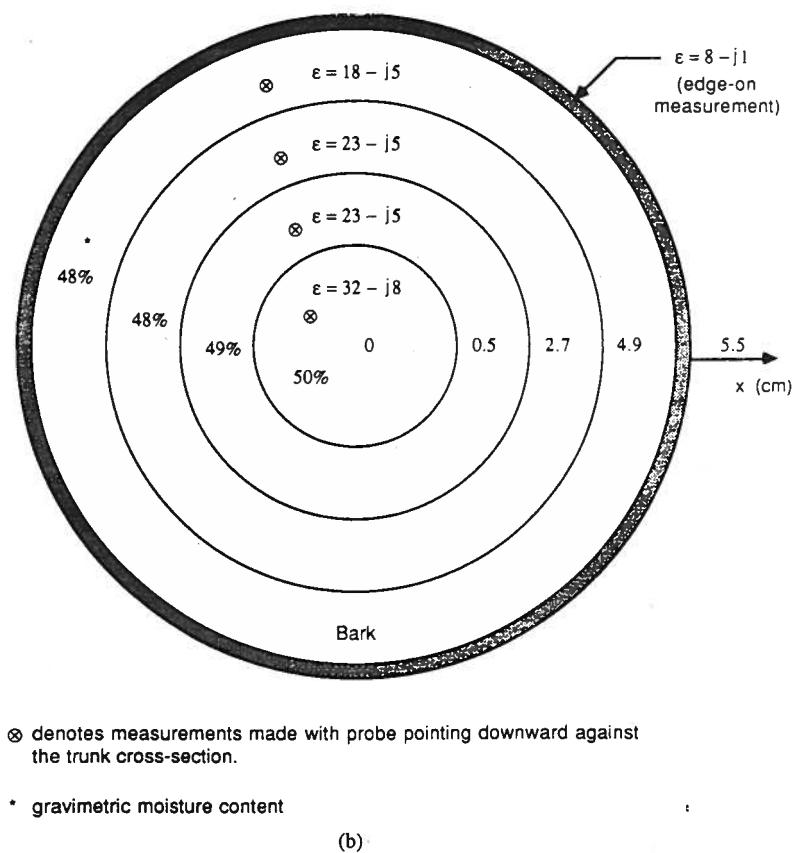
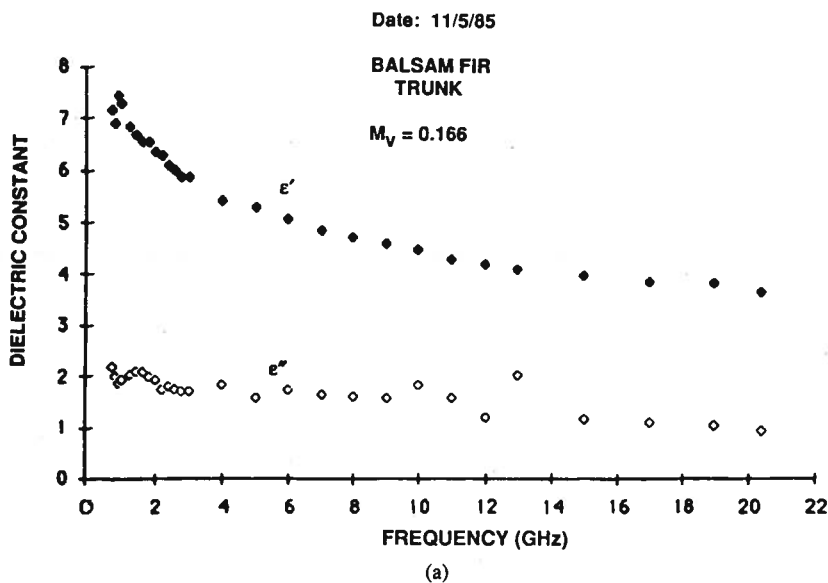
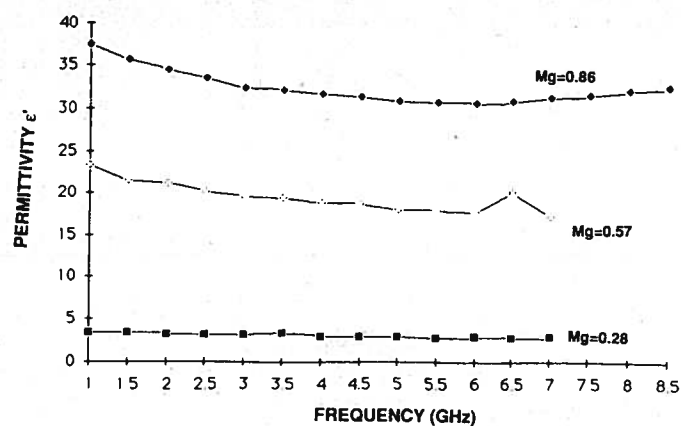


Fig. 7. Measured dielectric of the trunk of (a) a balsam fir tree and (b) a poplar tree.

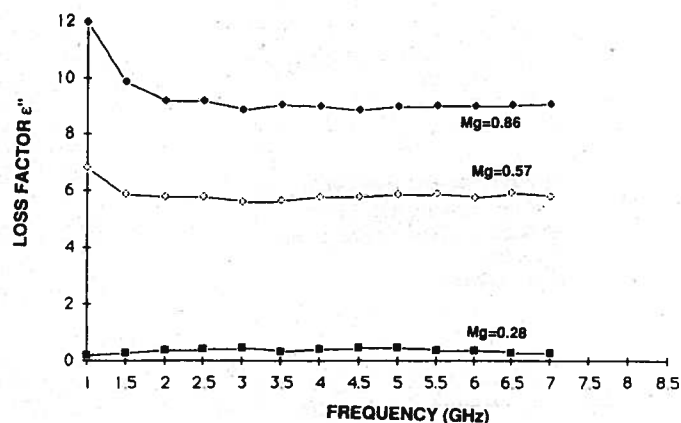
from a freshly cut corn stalk. Also shown is a theoretical spectrum calculated for a slightly saline water with a salinity of 7 percent. The expressions used are due to Stogryn [11] and are available in Ulaby *et al.* [8]. Overall, the measured spectrum is in very good agreement with the calculated spectrum. The deviation between the measured and calculated curves of  $\epsilon''$  above 12 GHz is attributed to multimode propagation.

#### IV. TEMPERATURE VARIATION

To evaluate the variation of  $\epsilon$  with temperature for vegetation material, use was made of a temperature chamber capable of operating over a wide range of temperatures both above and below freezing. A 2-m coaxial cable was used to connect the network analyzer system to the open-ended coaxial probe (which was placed inside the cham-



(a)

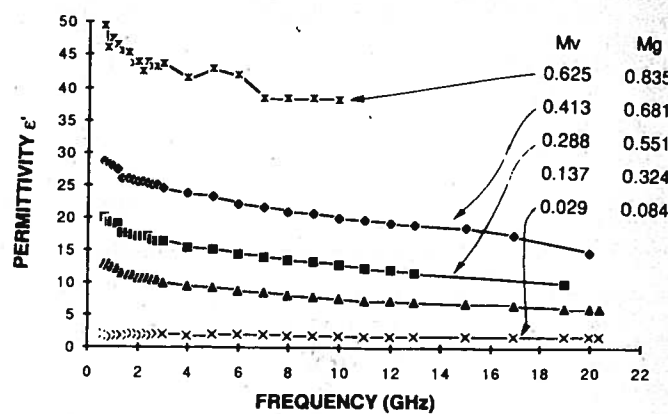


(b)

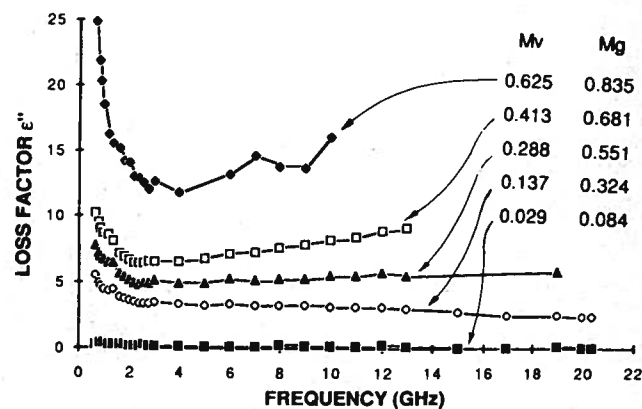
Fig. 8. Measured dielectric spectra of aspen leaves at three moisture conditions. (a)  $\epsilon'$ . (b)  $\epsilon''$ .

ber) through a special conduit in the wall of the chamber. The curves in Fig. 11 depict the variation of the dielectric constant of a corn leaf observed as the temperature was slowly lowered from room temperature at  $23^\circ\text{C}$  down to  $-32^\circ\text{C}$ . Our initial expectation was that the water in the leaves would freeze at a temperature somewhere between 0 and  $-1^\circ\text{C}$  because its salinity is on the order of 5‰ (the freezing temperature of liquid water with such a salinity is  $-0.3^\circ\text{C}$ ). The results shown in Fig. 11 suggest that the fluid in the corn leaf goes through a supercooling state down to about  $-6^\circ\text{C}$  and then it freezes instantaneously.

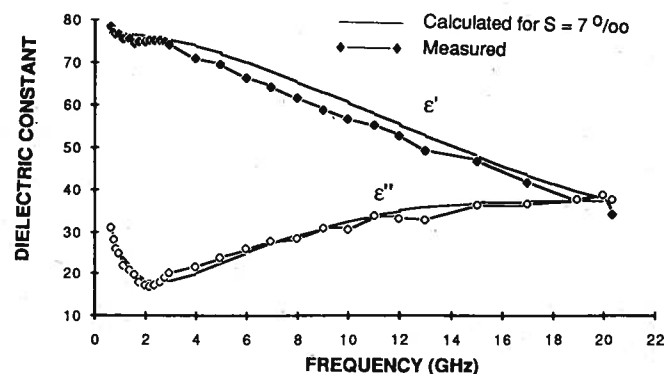
This temperature behavior was explored further by measuring  $\epsilon$  as a function of temperature during three consecutive half-cycles, as shown in Fig. 12. At the start of the experiment, the sample was at  $22^\circ\text{C}$ ; a freezing half-cycle was conducted during which the temperature dropped down to  $-32^\circ\text{C}$ ; the temperature was then raised slowly up to  $+3^\circ\text{C}$  (this half cycle is labeled "thawing" in the figure); and finally in the last half-cycle the temperature was made to drop again to well below freezing (ending at  $-15^\circ\text{C}$ ). There are two major observations worth noting. First, at the end of the first full cycle when the temperature reached  $+3^\circ\text{C}$ , the dielectric constant was (23-j13), compared to approximately (35-j21) at the same temperature during the first half-cycle. This differ-



(a)



(b)

Fig. 9. Family of dielectric spectra for corn leaves at various levels of moisture content. (a)  $\epsilon'$ . (b)  $\epsilon''$ .  $T = 22^\circ\text{C}$ .Fig. 10. Measured ( $\diamond$  and  $\blacklozenge$ ) dielectric spectrum of the fluid extracted from corn stalks, and calculated spectrum of saline water (—).

ence in level is partly explainable by the loss of moisture during the thawing cycle; the moisture content was 0.83 at the start of the experiment and 0.78 at the end of the first full cycle. Second,  $\epsilon$  exhibits a hysteresis-like effect as a function of the temperature  $T$ . This behavior, which was observed in this and numerous other experiments conducted for plant material at various levels of moisture content, may be related to the occurrence of some damage of the leaf cells due to water crystallization, but no adequate explanation is available at this time.



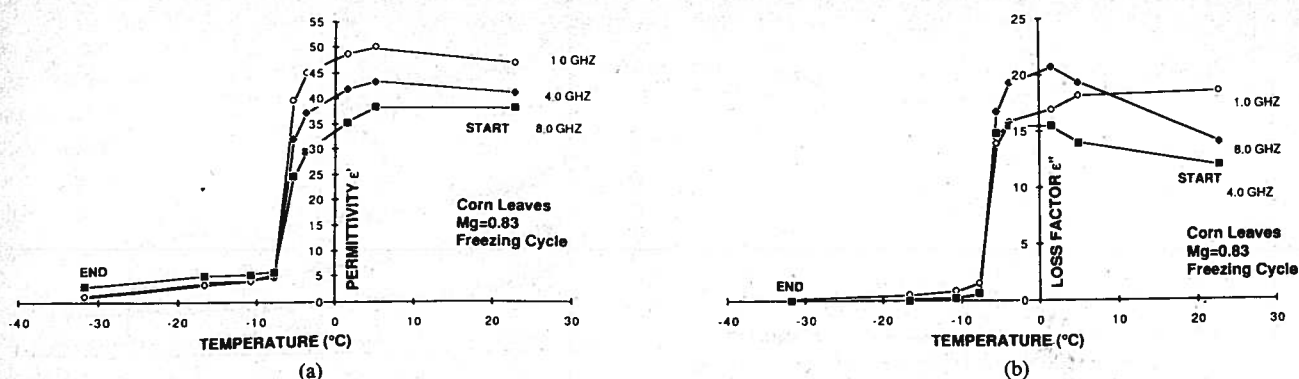


Fig. 11. Variation of  $\epsilon$  of corn leaves with decreasing temperature from 22 down to  $-32^{\circ}\text{C}$ . (a)  $\epsilon'$ . (b)  $\epsilon''$ .

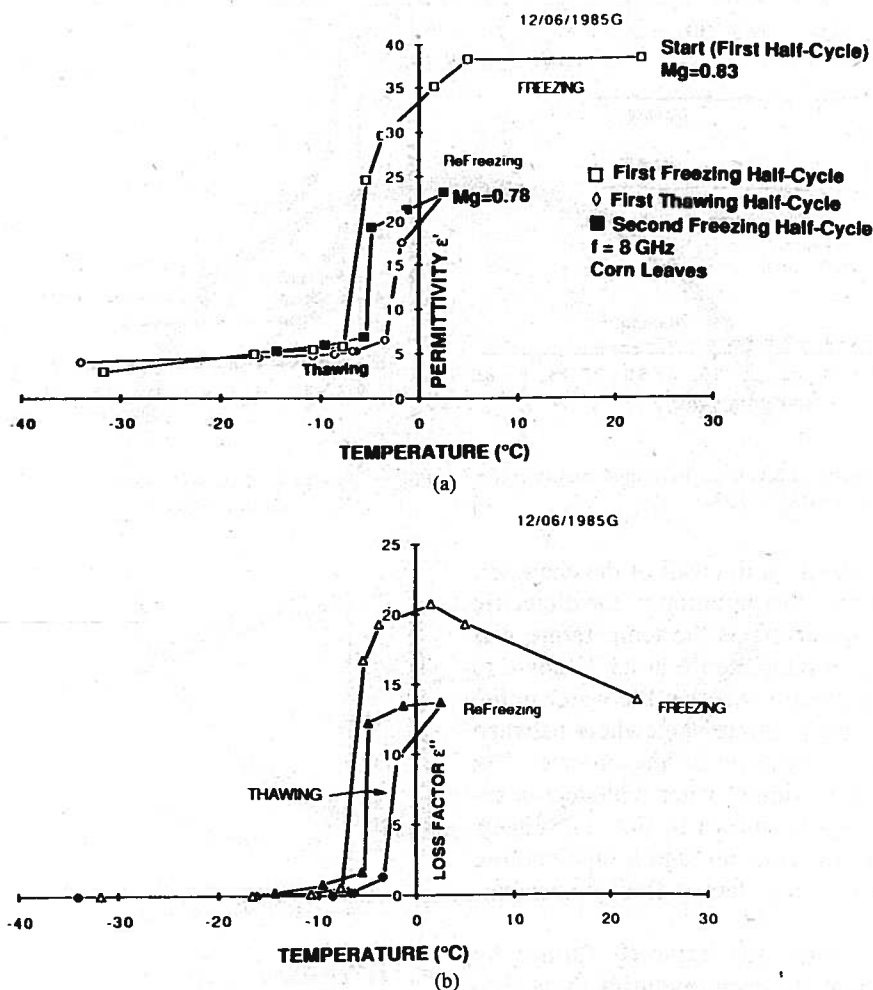


Fig. 12. Hysteresis-like behavior of the dielectric constant of vegetation as a function of temperature. (a)  $\epsilon'$ . (b)  $\epsilon''$ .

## V. CONCLUSION

The coaxial probe technique proved to be an extremely useful tool for making broad frequency dielectric measurements of vegetation material. Compared to the waveguide transmission technique used previously by one of the authors [1], the coaxial probe technique is far more accurate, more convenient to use, and an experiment that used to require a full week of work to conduct with the waveguide system now can be completed in about 30 min.

Already, the coaxial probe employed in this study has acquired more microwave dielectric data of vegetation material than all other previously published reports combined.

## REFERENCES

- [1] F. T. Ulaby and R. P. Jedlicka, "Microwave dielectric properties of plant materials," *IEEE Trans. Geosci. Remote Sensing*, vol. GE-22, pp. 406-414, 1984.
- [2] A. K. Fung and F. T. Ulaby, "A scatter model for leafy vegetation,"



- IEEE Trans. Geosci. Electron.*, vol. GE-16, no. 4, pp. 281–286, Oct. 1978.
- [3] M. A. Stuchly, T. W. Athey, G. M. Samaras, and G. E. Taylor, "Measurement of radio frequency permittivity of biological tissues with an open-ended coaxial line: Part II. Experimental results," *IEEE Trans. Microwave Theory Tech.*, vol. MTT-30, no. 1, pp. 87–92, Jan. 1982.
- [4] E. C. Burdette, F. L. Cain, and J. Seals, "In Vivo probe measurement technique for determining dielectric properties at VHF through microwave frequencies," *IEEE Trans. Microwave Theory Tech.*, vol. MTT-28, no. 4, pp. 414–427, Apr. 1980.
- [5] T. W. Athey, M. A. Stuchly, and S. S. Stuchly, "Measurement of radio frequency permittivity of biological tissues with an open-ended coaxial line: Part I," *IEEE Trans. Microwave Theory Tech.*, vol. MTT-30, no. 1, pp. 82–86, Jan. 1982.
- [6] N. Marcuvitz, *Waveguide Handbook*. New York, Dover, 1965.
- [7] G. A. Deschamps, "Impedance of antenna in a conducting medium," *IRE Trans. Antennas Propagat.*, pp. 648–650, Sept. 1962.
- [8] F. T. Ulaby, R. K. Moore, and A. K. Fung, *Microwave Remote Sensing*, vol. 3. Dedham, MA: Artech, 1986, Appendix E.
- [9] B. P. Jordan, R. J. Sheppard, and S. Szwarnowski, "The dielectric properties of formamide, ethanediol, and methanol," *J. Phys. D: Appl. Phys.*, vol. 11, 1978.
- [10] A. M. Bottreau, Y. D. Dutuit, and J. Moreau, "On multiple reflection time domain method in dielectric spectroscopy: Application to the study of some normal primary alcohols," *J. Chem. Phys.*, vol. 66, no. 8, Apr. 15, 1977.
- [11] A. Stogryn, "Equation for calculating the dielectric constant of saline water," *IEEE Trans. Microwave Theory Tech.*, vol. MTT-19, pp. 733–736, 1971.

\*

**Mohamed A. El-Rayes** was born in Cairo, Egypt, on November 4, 1952. He received the B.S. degree in electrical engineering from Ain Shams University, Cairo, Egypt, in 1975, the M.S. degree in microwave engineering

in 1979 from Kent University, Canterbury, England, and the Ph.D. degree from the University of Kansas in 1986. His research involves the measurement and modeling of vegetation materials at microwave frequencies.

\*



**Fawwaz T. Ulaby** (M'68–SM'74–F'80) was born in Damascus, Syria, on February 4, 1943. He received the B.S. degree in physics from the American University of Beirut, Lebanon, in 1964 and the M.S.E.E. and Ph.D. degrees in electrical engineering from the University of Texas, Austin, in 1966 and 1968, respectively.

From 1968 to 1984, he was with the Electrical Engineering Department at the University of Kansas, where he was the J. L. Constant Distinguished Professor, and the University of Kansas Center for Research, where he was Director of the Remote Sensing Laboratory. He is currently Professor of Electrical Engineering and Computer Science, The University of Michigan, Ann Arbor. His current research interests involve microwave propagation and active and passive microwave remote sensing. Along with R. K. More and A. K. Fung, he is a coauthor of the three-volume series *Microwave Remote Sensing: Active and Passive*, (Reading, MA: Addison-Wesley). In addition, he is coeditor of the *Manual of Remote Sensing*, 2nd ed., vol. 1 (American Society of Photogrammetry).

Dr. Ulaby is a member of Eta Kappa Nu, Tau Beta Pi, and Sigma Xi. He is the Executive Editor for the IEEE TRANSACTIONS ON GEOSCIENCE AND REMOTE SENSING, 1984–1988, and was the Geoscience and Remote Sensing Society's Distinguished Lecturer for 1986–1987. He received the GRS Society's Outstanding Service Award in 1982, and its Distinguished Service Award in 1983. In 1984, he also received a Presidential Citation for Meritorious service from the American Service of Photogrammetry and the IEEE Centennial Medal. He received the University of Kansas Chancellor's Award for Excellence in Teaching in 1980, the University of Kansas Gould Award for "distinguished service to higher education" in 1973, and the Eta Kappa Nu MacDonald award as an "outstanding electrical engineering professor in the United States of America" in 1975, the University College of Engineering Research Excellence Award in 1986, and the Kuwait Prize in applied science for 1986.